Solidification and Thermal Performance Analysis of the Low Carbon Steel During the Continuous Casting Process

Sobhan Mosayebidorcheh[1,*] , Mofid Gorji-Bandpy[2]

[1] *PhD Candidate, Department of Mechanical Engineering, Babol University of Technology, Babol, Iran.*
[2] *Professor, Department of Mechanical Engineering, Babol University of Technology, Babol, Iran.*

ARTICLE INFO	ABSTRACT

The present paper evaluates the effect of the nozzle characteristics on the heat transfer and phase change of low carbon steel during the continuous casting process. A three-dimensional energy equation and a solidification model are used to derive the governing equation of the phase change and temperature distribution. A linear relation is obtained to predict the temperature-dependence of the solid volume fraction in the mentioned steel. An effective thermal conductivity is used to simulate the advection effects of the liquid steel. The effective heat capacity is assumed to model the phase change in the mushy zone. The predicted values of the model are compared with the experimental ones. The regression values confirm a good agreement between the modeled and experimental values. The effects of geometry of the slab and the secondary cooling characteristics are examined on the heat transfer and solidification of the steel slab. The slab thickness has a significant effect on the solidification and by increasing this parameter, the metallurgical length will increase.

1-Introduction

Continuous casting operation of steel extends several decades back to generate forms for further semi-fabrication processes such as rolling or extrusion. The forms of the productions usually include thick slabs (rectangular cross section with thickness between 50 and 300 millimeters and width between 900 and 2000 millimeters), billets (square cross section about 200 millimeters), thin slabs (thickness less than 75 millimeters), strip (thickness less than 12 millimeters), and round billets (diameter less than 500 millimeters). Recently, due to a significant increase in yield, energy saving and quality of the production, a growth of this technology has been identified in the steel companies. In this relation, the casting technique of steel alloy products has improved specific properties in terms of the casting process, machinery, and quality control methodologies.

The continuous casting process is controlled by some properties such as the casting speed and water flow rates in the secondary cooling zones. The higher speed and so higher production is always sought for. Anyway, the casting speed cannot be exceeded optionally for some reasons [1]. Increasing the casting speed causes the growing depth of liquid pool and also increasing the surface temperature of the slab. So, the cooling equipment is needed for secondary

* Corresponding author:
E-mail address: sobhanmosayebi@yahoo.com

cooling zones.

The continuous casting machinery includes two cooling sections: primary cooling in the mold and secondary cooling (see Fig. 1). The cooling systems are planned to extract the superheat from the entering liquid steel, latent heat of fusion at the solidification front, phase change energy and sensible heat from the solidified slab [2]. The thermal condition of the steel slab changes repeatedly due to the variations of the casting parameters. To control the thermal condition of steel slab, one way is dynamic control model [4-7]. Using the dynamic control tools, the physical parameters of continuous casting such as shell thickness, surface temperature, and metallurgical length can be estimated and controlled according to the immediate operating system.
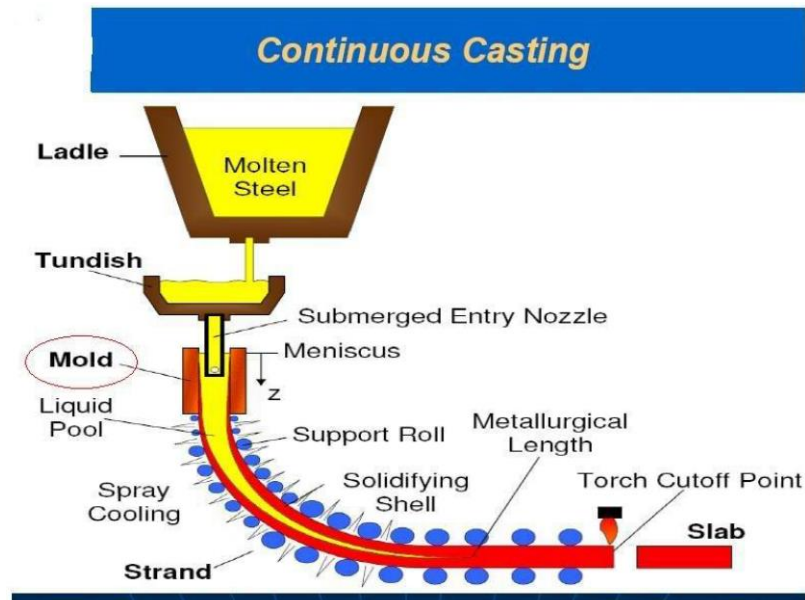

Fig. 1. Schematic diagram of continuous casting process [3].

Recently, two-dimensional and three dimensional thermal models are used in the dynamic control systems by Hardin et al. [8] and Spitzer et al. [9]. In the dynamic control models, it is hard to match the results of simulation and measurement in all times, but the model can be validated by experimental measurements for some special cases. The efficiency of the dynamic control systems can be considered by comparison of the real temperatures and predicted temperatures.
To have a well-operating efficiency, it is essential to monitor the surface temperature of the slab online and prepare the suitable feedback for spray water of secondary cooling. Water flow rates of secondary cooling are controlled pursuant to the temperature measurements in the casting line. Online control of strand temperature using the feedback of measured temperature have reported by Camisani-Calzolari et al. [10] and Chen and Cai [11].

The configuration of the nozzles, the values of water flow rate and control technique highly influence the behavior of the slab solidification. On the one hand, overcooling can cause to decrease the surface temperature to low ductility region, which can produce the cracks [12]. On the other hand, undercooling may lead to bulging or breakout in the strand [13]. In addition, inappropriate secondary cooling can result in the surface extreme reheating, which causes the surface and internal cracks [14]. Thus, the optimum design and control of water flow rates in the secondary cooling zones can better the strand quality by the minimization the temperature variations [15]. The velocity cascade control (VCC) technique [16, 17] is a kind of secondary cooling strategy where a quadratic relation is between the water flow rates and casting speed.

This controlling technique has been widely used in various industries and tallies with the theory and practice. Another controlling technique is the estimation of water flow rates of secondary cooling zones using the online temperature measurements of slab surfaces [8]. However, this strategy is usually unpractical

because it has some difficulties such as scale formation on the steel slab and presence of steam in the secondary cooling zones [19]. Lately, the dynamic secondary cooling techniques were used which are based on the real-time computation [20-23]. This method can compute the optimal water flow rate for each spray cooling zone according to the casting parameters such as the casting speed, the thickness of slab, the casting temperature, etc. Some modifications on the secondary cooling parameters of continuous casting have also been used such as neural networks [24], minimization of cost function [25-29], colony optimization [30], and multi-objective optimization [31, 32].

In this paper, the heat transfer and solidification of the steel slab are simulated during the continuous casting process. The simulated results are compared with the measurements for a special case. The effects of the characteristics of secondary cooling zones are investigated. These parameters are the nozzle angel, the height of the nozzles, and the flow rates of the secondary cooling zones. The optimum injection angles of the secondary cooling nozzles are obtained for slabs with different widths.

2- Governing heat flow equation

The continuous casting is a complex process and has various physical behaviors. Because of this, the researchers choose one issue related to this topic. One of the significant subjects of this process is the heat transfer and phase change. The thermal and solidification modeling impresses instantly on the other issues of continuous casting process. The following assumptions are utilized to derive the governing equations:

1- Conduction heat transfer in the casting direction is insignificant compared to the transverse shines.
2- Thermo-physical properties of the metal are varied as a function of temperature.
3- An equivalent specific heat capacity is employed for the change phase.
4- A corresponding thermal conductivity is used for considering the convection heat transfer of liquid steel and mushy zones.
5- The emissivity of the steel is supposed to be a function of temperature.
6- The liquid steel flow rate is fixed.

7- The surrounding temperature is supposed to be constant.
8- The roll contact is assumed to be constant.

Due to the assumptions, the heat transfer equation can be represented by:

$$\rho c_p \left(\frac{\partial T}{\partial t} + V_{Cast} \frac{\partial T}{\partial z} \right) = \frac{\partial}{\partial x}\left(k_{eff}(T)\frac{\partial T}{\partial x} \right) + \frac{\partial}{\partial y}\left(k_{eff}(T)\frac{\partial T}{\partial y} \right) + \dot{q}$$

where x, y are the transverse directions, c_p is the specific heat, T is the steel temperature, ρ is the density of steel, k_{eff} is the effective thermal conductivity, t is the time, z is direction along the casting, and $\dot{q}$ is the heat generation which caused by solidification. The first and second terms in the left side show the unsteady behavior of strand temperature and the transferred energy of casting steel, respectively. The transverse conduction heat transfer in the *x* and *y* directions is determined by the first two terms on the right hand of the above equation. Heat generation of solidification is expressed by the last term of the right hand side.

k_{eff} or effective thermal conductivity shows the increased value of heat transfer in the mushy zone and liquid phase due to the convection heat transfer [33].

The heat generation $\dot{q}$ in the energy equation (Eq. (1)) is related to the solid fraction of steel and by increasing the solid volume fraction, the heat generation will also increase.

$$\dot{q} = \Delta h \left(\frac{\partial(f_s \rho)}{\partial t} + V_{cast} \frac{\partial(f_s \rho)}{\partial z} \right)$$

where Δh is the latent heat of the steel. The solid volume fraction of steel can be determined from the solidus and liquidus temperatures. The most common equation for solid volume fraction is the following equation [34]:

$$f_{sol} = \begin{cases} 0 & T > T_{liq} \\ \dfrac{T_{liq} - T}{T_{liq} - T_{sol}} & T_{sol} \leq T \leq T_{liq} \\ 1 & T < T_{sol} \end{cases}$$

The continuous casting process has a complex behavior. It includes some kinds of thermal boundary conditions. Because of this, specifying the suitable thermal boundary conditions is difficult. Nevertheless, the scientists have used some formulations for different types of heat transfer. These formulations can be employed due to the

engineering applications.

Primary cooling in the mold has significant effects due to making an initial solid steel shell around the strand. The thickness of the steel shell at the end of the mold must be a minimum value to prevent the break-out phenomenon. The primary cooling in the mold section is included by:

- Convection heat transfer of liquid metal to the slab surface,
- Solidification of liquid metal in the mushy region,
- Conduction heat transfer in the solid shell,
- The characteristics of supplies between the strand and the mold,
- Conduction heat transfer in the mold,
- Forced convection heat transfer between the cooling water and the copper mold.

The mean heat transfer in the mold can be computed by the temperature difference between the inlet and outlet of cooling water in the mold and the flow rate of the cooling water [35].

$$\bar{q} = \frac{c_w Q_m \Delta T_w}{S_{eff}}$$

where c_w is the specific heat capacity of the cooling water, ΔT_w is the temperature difference between the inlet and outlet of the cooling water, Q_m is the cooling water flow rate, S_{eff} is the area of the interface between the mold and the steel and $\bar{q}$ is the mean heat flux from the mold.

The heat flux distribution along the casting direction can be presented by the following equation:

$$q(z) = 2680000 - \beta \left(\frac{z}{V_{cast}}\right)^{1/2}, \quad \beta = \frac{1.5(2680000 - \bar{q})}{\left(\frac{L_m}{V_{cast}}\right)^{1/2}}$$

where $q(z)$ is the heat flux distribution and L_m is the mold length.

The thermal boundary condition in the secondary cooling zones can be represented by the following equation:

$$-k_{steel} \frac{\partial T_s}{\partial n} = h(T_s - T_{amb})$$

where T_{amb} is the ambient temperature and h is the equivalent heat transfer coefficient corresponding to the radiation cooling, heat conduction to the rolls, the spray nozzle cooling, and natural heat convection (see Fig. 2). The heat losses of the strand in the secondary cooling zone can be modeled by the above thermal conditions.
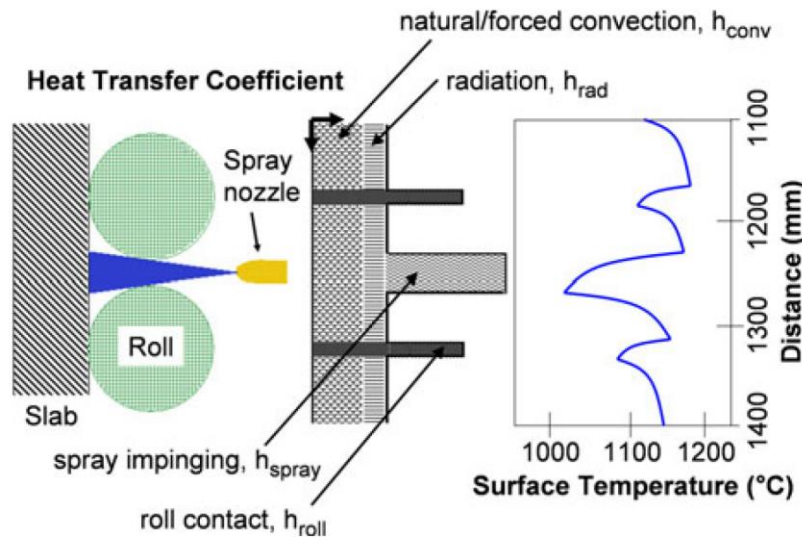

Fig. 2. Schematic diagram of secondary cooling zone [36].

The heat transfer coefficient and heat losses of spray cooling are related to the temperature of cooling water and water flow rate of the nozzles [37]:

$$h_{spray} = A \times Q_{sw}^c \times (1 - b \times T_{spray})$$

where Q_{sw} is the water flow rate, T_{spray} is the temperature of the cooling water. Some scientists attempted to determine the parameters of the above equations using the experimental measurements. Nozaki [38] has determined the following values for Eq. (7):
$A = 0.3925$, $c = 0.55$, $b = 0.0075$

In addition, some works studied the heat losses of the nozzles due to the properties of nozzles such as the flow rate of the nozzle, the space between the nozzles, the type of the nozzle and the distance between the nozzle and strand surface [39, 40]. Heat transfer coefficient of the spray nozzles must be modified for the downward facing surface to include the effect of orientation [41].

$$h_{spray, bottom face} = (1 - 0.15 \cos \theta) h_{spray, top face}$$

where θ is the angle of strand from horizontal direction and $h_{spray, bottom face}$ and $h_{spray, top face}$ are the convection heat transfer coefficients of the spray nozzles in the bottom face and top face of strand, respectively.

The strand surfaces except roll contacts extracted heat by radiation mechanism.
The emissivity of the steel has the following temperature-dependent relation [42].

$$\varepsilon = \frac{0.85}{\left[1 + \exp\left(42.6 - 0.02682 T_{surface} \right)^{0.0115} \right]}$$

where $T_{surface}$ is the surface temperature. The equivalent heat transfer coefficient for the radiant heat transfer can be employed:

$$h_{rad} = \varepsilon \sigma \left(T_{surface}^2 + T_{ambient}^2 \right) \left(T_{surface} + T_{ambient} \right)$$

where σ is Stefan–Boltzmann constant $\left[5.67 \times 10^{-8} W / m^2 K^4 \right]$.

The heat loss from the roll contacts has been obtained using the measurements in the experimental studies. The contact length of rolls is about 20 percent of the roll radius. The following relation can be employed for the heat flux of the roll contact as a function of the slab surface temperature, the casting speed and the arc of the roller contact:

$$q''_{roll} = 11513.7 \times T_{surface}^{0.76} \times V_{casting}^{-0.2} \times (2\theta)^{-0.16}$$

where θ is the angle of the roller contact in degree and q''_{roll} is the heat flux of roll contact. The natural convection as another type of heat transfer which can be computed by [41]:

$$h_{nat} = 0.84 \left(T_{surface} - T_{ambient} \right)^{\frac{1}{3}}$$

where h_{nat} is the heat transfer coefficient of natural convection.

The heat transfer coefficients of all regions will apply to the local parts for each kind of heat transfer. Due to excessive changes in the heat transfer coefficient along the casting direction, the slab surface temperature will be sinusoidal. Due to this behavior, it is difficult to have a comprehensive study on this kind of the results. Hence, the following weighted-area average heat transfer coefficient is used for each secondary cooling zone [43]:

$$h_{ave} = \frac{h_{roll} A_{roll} + h_{nat} A_{nat} + h_{rad} A_{rad} + h_{spray} A_{spray}}{A_{tot}}$$

where h_{ave} is the weighted-area average heat transfer coefficient, h_{nat}, h_{rad}, h_{roll}, and h_{spray} are the equivalent heat transfer coefficient of natural convection heat transfer, equivalent radiation heat transfer coefficient, roll contact and spray cooling heat transfer coefficient, respectively. A_{nat}, A_{roll}, A_{spray}, A_{rad} and A_{tot} are the natural convection area, contact roll area, spray cooling area, radiation heat transfer area and total area, respectively.

3- Numerical method
In this paper, the Euler view point is used to solve the energy equation for the strand. It uses a computational real coordinate for the strand geometry. The numerical method which can be employed for this problem is the finite volume method (FVM). The steady state heat transfer equation can be represented by:

$$div \left(\rho u T \right) = div \left(k \; grad \, T \right) + S_T$$

where S_T is the source term which is temperature dependent. The integral form of control volume is

$$div \left(\rho u T \right) = div \left(k \; grad \, T \right) + S_T$$

where n and A are normal vector of corresponding surface and the surface of control volume, respectively. The details of the numerical discretization have been presented in the paper [44].

4- Results and discussion
To validate the present model, empirical measurements in the continuous casting

companies are required. The characteristics of the secondary cooling zones were presented in previous sections. In addition to the above mentioned information, other information is used in simulation and modeling of the solidification which is not presented here. Some of this information contains the items such as: the casting machine characteristics (dimensions and curvatures of the machine), the mold length and width, the number of secondary cooling zones, guide rollers properties (number, type, position and distance between adjacent rollers), cooling nozzle properties in every cooling zone (number, type, vertical distance to the strand, injection angle, nozzle spacing from each other, nozzles type). In addition, there are some other properties which must be determined in steel company during the production that contains: solidus temperature, liquidus temperature, casting temperature, slab dimensions (thickness and width), casting velocity, water flow rate and its temperature variation of the mold. The temperature of the strand surface must be measured using pyrometer in different points.

In this section, the simulation results are presented and discussed. Firstly, the solution procedure is provided and an initial temperature field is assumed for the strand. Then it is substituted in the heat transfer equation. By solving the heat transfer equation in each step, the temperature distribution is obtained and temperature-dependent physical properties such as effective thermal conductivity can be computed. The boundary conditions of heat transfer equation are applied on the mold section and secondary cooling zones.

Solidification and temperature distribution in continuous casting of steel are the worthwhile results of the present work which can be drawn with two strategies: using the local and area-averaged heat transfer coefficients.

The first strategy considers the heat transfer of the strand as well as a minor point of view while the second strategy uses an area-weighted treatment for analyzing the heat transfer.

Here, 3 different states are considered as well as the base states. These base items have different widths: 1160 mm, 1540 mm, and 1880 mm. The parameters and casting characteristics of each state are presented in the Tables 4, 5 and 6 for the width of 1160 mm, 1540 mm, and 1880 mm, respectively.

Fig. 3 shows the comparison between the simulation results and experimental measurements for the case width 1540 mm.
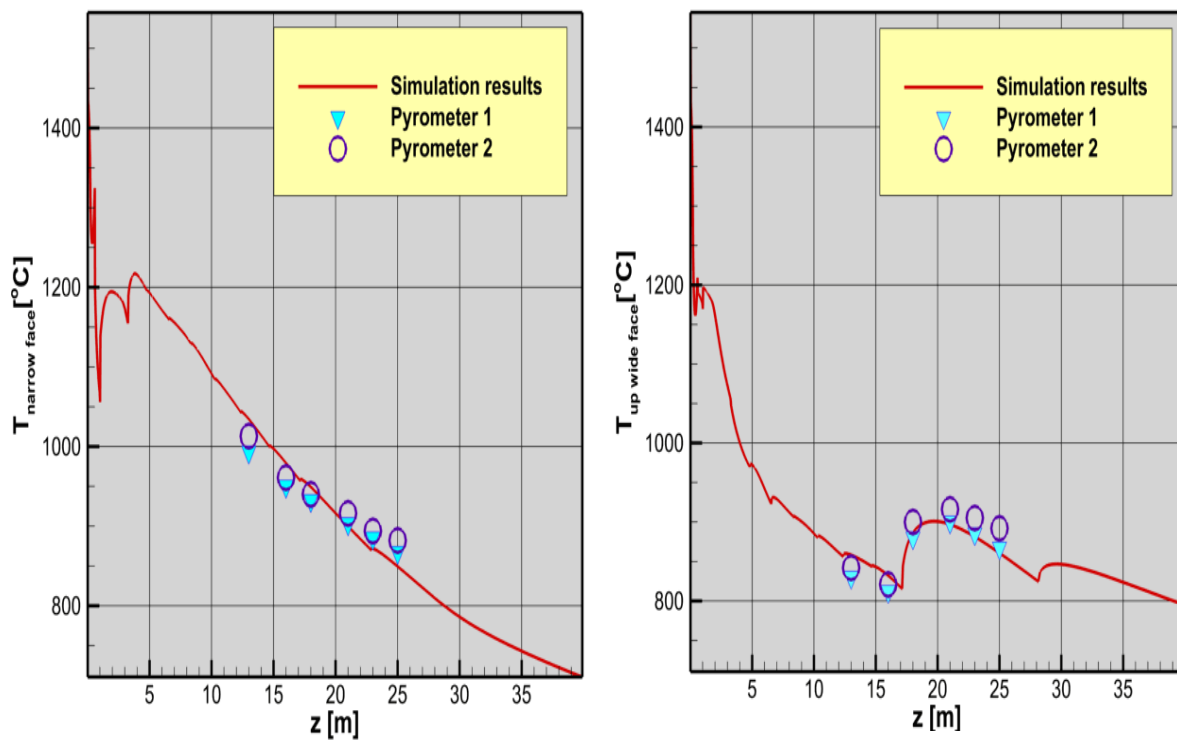

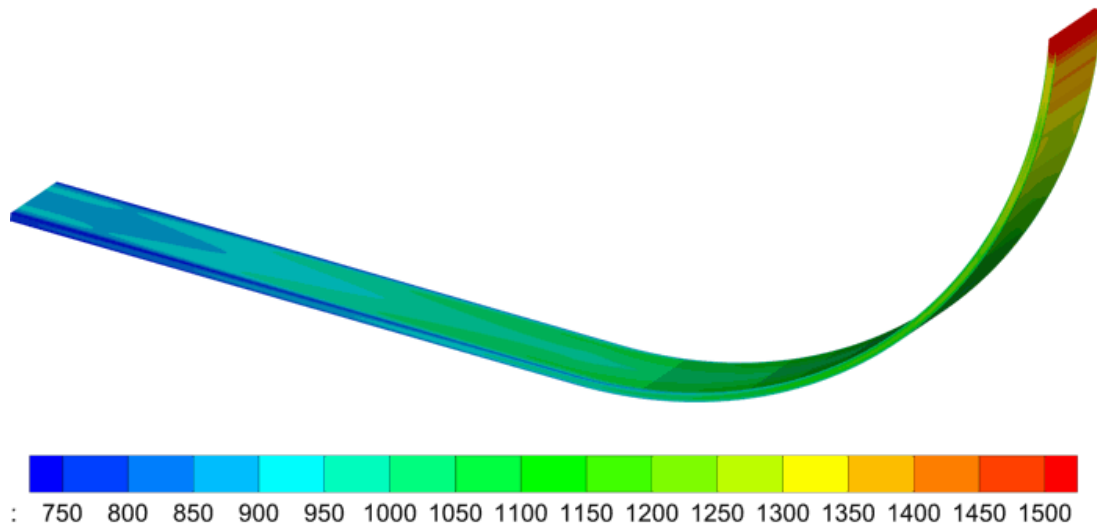**Fig. 3.** The comparison of simulation results and temperature measurements.

Fig. 4. The 3D temperature contour of steel slab for the strand with width 1880 mm.

As can be seen in Fig. 3, the simulation results are in good agreement with the empirical measurements. The root mean square deviation (RMSD) of the obtained results is about 17 °C based on the following relation:

$$RSMD = \sqrt{\frac{\sum_{i=1}^{n}\left(T_{Measure} - T_{simulate}\right)^2}{n}}$$

where $T_{Measure}$ is the measurement temperatures in the casting line, $T_{simulate}$ is the simulated temperatures and n is the number of the measurements. The graphical results of simulation are presented in the Figs. 4 to 7. The 3D contour of the strand temperature is shown in Fig. 4.

Fig. 5 shows the effects of the thickness of steel slab on the growth of solid thickness around the wide face. As can be seen, the thickness of the slab has a great effect on the solid thickness value. By changing the slab thickness from 200 mm to 300 mm, the metallurgical length increases from 14.3 m to 30.8 m. So, increasing the water flow rates in the secondary cooling is needed to keep the metallurgical length in a constant range for high thickness slabs.

Fig. 6 shows the temperature distribution of the slab center for different values of tundish temperature. The distance to the mushy zone is more for the high tundish temperatures. Although the tundish temperature has no significant effect on the metallurgical length, but it can be predicted that by increasing the casting velocity, the impact of tundish temperature will increase.

Fig. 7 shows the temperature of the slab center for different slab widths. In the first casting line, the temperature of the slab center decreases to the liquidus temperature, rapidly and then it is reduced by a slow gradient in the mushy zone to reach solidus temperature. In the solid phase zone, the value of temperature gradient increases. The slow temperature gradient in the mushy zone is because of the high latent heat of steel. In other word, the effective specific heat of steel in this region is a high value and so the steel slab in this zone must be cooled more than the other zones.
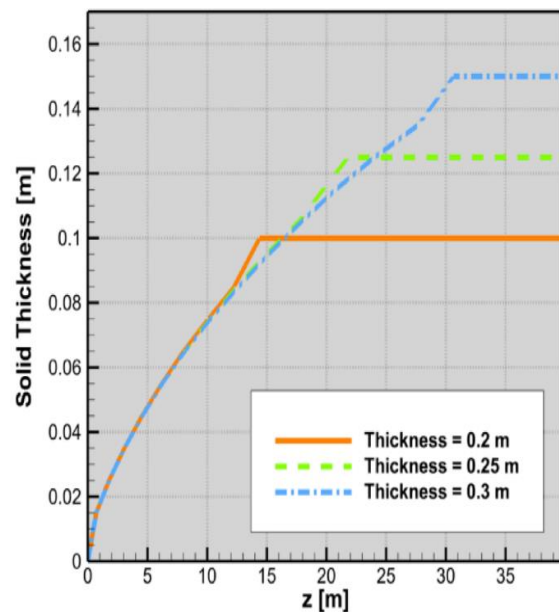

Fig. 5. The solid thickness of the steel around the wide face for the different values of thickness when width= 1880 mm.
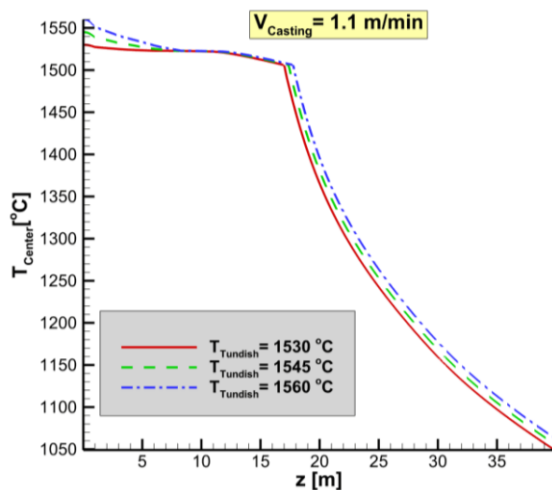
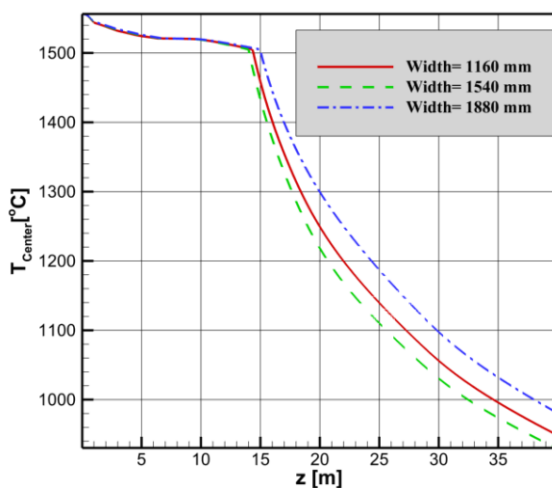**Fig. 6.** The temperature of slab center for different values of tundish temperature for width 1880 mm.

Fig. 7. Temperature distribution of slab center for different slab widths.

5- Conclusions

This work studied and analyzed the heat transfer and solidification of the steel slab in the continuous casting process. The governing equations are derived based on a three-dimensional model of energy balance for the strand. The solid volume fraction and shell thickness of the steel are obtained using a linear temperature-dependent relation. The simulation results are compared with the experimental measurements. The effects of geometry of the slab and the secondary cooling characteristics are examined on the heat transfer and solidification of the steel slab. The slab thickness has a significant effect on the solidification and by increasing this parameter, the metallurgical length will increase.

References

[1] C. Li and B.G. Thomas, "Proceedings of the Brimacombe Memorial Symposium, Vancouver, 2000, TMS, Warrendale, p. 595.

[2] J. Sengupta, B.G. Thomas, M.A. Wells, "The Use of Water Cooling during the Continuous Casting of Steel and Aluminum Alloys", Met. Trans. A, Vol. 36, 2005, p. 187.

[3] Continuous Casting Consortium, ccc.illinois.edu.

[4] B. G. Thomas, J. Bentsman, K. Zheng, S. Vapalahti, B. Petrus, J. Kim, A. K. Behera, A. H. Castillejos and F. A. Acosta, Proc. Conf. 2006 NSF Design, Service, and Manufacturing Grantees and Research: 'Online dynamic control of cooling in continuous casting of thin steel slabs', 1–11; 2006, St Louis, MO, National Science Foundation.

[5] J. Ma, Z. Xie and G. Jia: 'Applying of real-time heat transfer and solidification model on the dynamic control system of billet continuous casting', ISIJ Int., 2008, 48, (12), 1722–1727.

[6] S. Louhenkilpi, E. Laitinen and R. Nieminen: 'Real-time simula- tion of heat transfer in continuous casting', Metall. Trans. B, 1993, 24B, 685–693.

[7] J. Chen and B. Fan: 'Survey of the dynamic control of secondary cooling', Bao Steel Technol., 2000, 4, 37–39.

[8] R. A. Hardin, K. Liu, C. Beckermann and A. Kapoor: 'A transient simulation and dynamic spray cooling control model for continuous steel casting', Metall. Mater. Trans. B, 2003, 34B, 297–306.

[9] K. H. Spitzer, K. Harster, B. Weber, P. Monheim and K. Schwerdtfeger: 'Mathematical model for tracking and on-line control in continuous casting', ISIJ Int., 1992, 32, (7), 848–856.

[10] F. R. Camisani-Calzolari, I. K. Craig and P. C. Pistorius: 'Speed disturbance compensation in the secondary cooling zone in continuous casting', ISIJ Int., 2000, 40, (5), 469–477.

[11] S. Chen and K. Cai: 'Secondary cooling water control model for slab continuous caster', Steelmaking, 1994, 4, 30–35.

[12] S. Mazumdar, S. K. Ray, Solidification control in continuous casting of steel, Sadhana, 26 (2001), No. 1-2, 179.

[13] J. S. Ha, J. R. Choa, B. Y. Lee, M. Y. Ha, Numerical analysis of secondary cooling and bulging in the continuous casting of slabs, J. Mater. Process Tech, 113 (2001), No. 1-3, 257.

[14] J. K. Brimacombe: Can. Metall. Q, 15 (1976), No. 2, 163.

[15] J. Zhang, D. Chen, S. Wang, M Long,

Compensation Control Model of Superheat and Cooling Water Temperature for Secondary Cooling of Continuous Casting, steel research int. 82 (2011) No. 3.

[16] K. Inazaki, M. Takahashi, Y. Chida, M. Yamamoto, H. Kawataka, N. Nakano, T. Tagami: Trans. ISIJ, 24 (1984), No. 1, 75.

[17] Y. Liu, T. M. Cao, A. M. Xi: J. Univ. Sci. Technol. Beijing, 28 (2006), No. 3, 290.

[18] Z. P. Ji, Z. Xie, Z. Y. Lai: Information and Control, 37 (2008), No. 5, 576.

[19] F. R. Camisani-calzolari, I. K. Craig, P. C. Pistorius: ISIJ Int., 40 (2000), No. 5, 469.

[20] R. A. Hardin, K. Liu, A. Kapoor, C. Beckermann: Metall. Mater. Trans. B, 34B (2003), 297.

[21] W. H. Liu, Z. Xie, Z. P. Ji, B. Wang, Z. Y. Lai, G. L. Jia: J. Iron Steel Res. Int., 15 (2008), No. 2, 14.

[22] S. Louhenkilpi, E. Laitinen, R. Nieminen: Metall. Mater. Trans. B, 24B (1993), 685.

[23] J. C. Ma, Z. Xie, G. L. Jia: ISIJ Int., 48 (2008), No. 12, 1722.

[24] B. Salah, L. Malek, B. Ja¨urgen: Acta Automatica Sinica, 34 (2008), No. 6, 701.

[25] D. deV. van der Spuy, I. K. Craig, P. C. Pistorius: The Journal of The
South African Institute of Mining and Metallurgy, (1999), 49.

[26] F. R. Camisani-Calzolari, I. K. Craig, P. C. Pistorius: ISIJ Int., 38 (1998), No. 5, 447.

[27] A. V. Lotov, G. K. Kamenev, V. E. Berezkin, K. Miettinen: Appl. Math. Model, 29 (2005), No. 7, 653.

[28] B. Z. Guo, B. Sun: J Global. Optim, 39 (2007), No. 2, 171.

[29] P. Zheng, J. Guo, X. J. Hao: Hybrid Strategies for Optimizing Continuous Casting Process of Steel. IEEE ICIT-04 Proc. (2004), Vol. 3, p. 1156.

[30] Z. P. Ji, B. Wang, Z. Xie, Z. Y. Lai: Ant colony optimization based heat transfer coefficient identification for secondary cooling zone of continuous caster, IEEE ICIT-07 Proc. 2007, p. 558.

[31] K. Miettinen: Mater. Manuf. PROCESS, 22 (2007), No. 5, 585.

[32] Z. P. Ji, Z. Xie: Multi-objective Optimization of Continuous Casting Billet Based on Ant Colony system Algorithm, IEEE PACIIA-08 Proc., 2008, Vol. 1, p. 262.

[33] J. Zhang, D. Chen, S. Wang, M. Long, Compensation Control Model of Superheat and Cooling Water Temperature for Secondary Cooling of Continuous Casting, steel research

international. 82 (2011) No. 3.

[34] H. Wang, G. Li, Y. Lei, Y. Zhao, Q. Dai, J. Wang, Mathematical Heat Transfer Model Research for the Improvement of Continuous Casting Slab Temperature, The Iron and Steel Institute of Japan International, Vol. 45 (2005), No. 9, pp. 1291–1296.

[35] X. Y. Wang, Q. Liu, B. Wang, X. Wang, J. S. Oing, Z. G. Hu, H. Sun, Optimal control of secondary cooling for medium thickness slab continuous casting, Ironmaking and Steelmaking, (2011), VOL 38, NO 7.

[36] B. Petrus, K. Zheng, X. Zhou, B. G. Thomas, J. Bentsman, Real-Time, Model-Based Spray-Cooling Control System for Steel Continuous Casting, Metallurgical and Materials Transactions B, Volume 42B, February 2011—87.

[37] J.K. Brimacombe, P.K. Agarwal, S. Hibbins, B. Prabhaker, and L.A. Baptista: in Continuous Casting, J.K. Brimacombe, ed., (1984), vol. 2, pp. 105–23.

[38] Nozaki, T., Matsuno, J., Murata, K., Ooi, H., Kodama, M., A Secondary Cooling Pattern for Preventing Surface Cracks of Continuous Casting Slab‖, Transactions of the Iron and Steel Institute of Japan, V. 18, 1978, pp.330-338.

[39] E.A. Mizikar, Mathematical heat transfer model for solidification of continuously cast steel slabs, AIME Transactions of the Metallurgical Society, (1967) 1747–1758.

[40] L.K. Chiang: Proc. 57th Electric Furnace Conf., Pittsburgh, PA, 1999.

[41] R. A. Hardin, K. Liu, Atul Kapoor, C. Beckermann, A Transient Simulation and Dynamic Spray Cooling Control Model for Continuous Steel Casting, Metallurgical and Transactions B, Volume 34B, (2003)-297.

[42] Y.S. Touloulian, R.W. Powell, C.Y. Ho, and P.B. Klemens, Thermophysical Properties of Matter, IFI/Plenum, New York, NY, (1972), vol. 8.

[43] L. Guo, Y. Tian, M. Yao, and H. Shen, Temperature distribution and dynamic control of secondary cooling in slab continuous casting, International Journal of Minerals, Metallurgy and Materials Volume 16, Number 6, (2009), 626.

[44] S. Mosayebidorcheh, M. Gorji-Bandpy, Local and averaged-area analysis of steel slab heat transfer and phase change in continuous casting process, Applied Thermal Engineering 118 (2017), 724-733.